Mater Renew Sustain Energy (2014) 3:29
DOI 10.1007/s40243-014-0029-2

ORIGINAL PAPER

Trials for oxide photo-thermoelectrics

Ichiro Terasaki · Ryuji Okazaki · Partha Sarathi Mondal · Yu-Chin Hsieh

Received: 18 February 2014 / Accepted: 4 April 2014 / Published online: 1 May 2014

Abstract Thermoelectrics is an energy conversion technology from heat into electricity, and vice versa, through the thermoelectric phenomena in solids, while photovoltaics is an energy conversion technology from solar photon energy into electricity using the photo-excitations in solids. We are trying to find a way to combine thermoelectrics with photovoltaics to establish a new method to generate renewable energy with high efficiency. In this article, we show two approaches for this purpose using oxide materials: thermoelectric energy conversion by photo-excited carriers and the thermoelectric power generation using a focused light as a heat source.

Keywords Thermoelectric power generation · Oxide · Photo-doping · Photo-thermoelectrics

Introduction

No one can deny that our modern society is based on vast consumption of electric/chemical energies. Since all the developing countries have the right to enjoy life as comfortable as the advanced countries do, energy demands are increasing year by year in spite of serious shortage of petroleum. Thus, a search for sufficient energy resources is a responsibility of researchers in all areas of science and technology. Best energy resources are of no doubt renewable energies, which preliminarily come from the solar energy.

The energy conversion technique using the solar energy is classified into two; The one is photovoltaics in which an electron–hole pair created by an incident photon is separated by an internal electric field at the *p*–*n* junction [27]. This technology is now commercially available as solar battery cells. The other is solar-thermal energy conversion, where heat generated by focused sunlight vaporizes water to rotate a gas turbine [34]. Although these two techniques are matured, there remain issues to be addressed. In photovoltaics, the conversion efficiency is close to a theoretical limit, and raw materials of silicon of high quality are about to run out. Of course alternative materials are being developed, but the cost and natural abundance are still issues. In the case of solar-thermal conversion, the conversion efficiency is not satisfactory except for some areas around the equators.

We have studied thermoelectric energy conversion using oxide materials, which are superior at high temperatures in air [9, 13]. A serious drawback of thermoelectrics is poor efficiency [28]. A good thermoelectric material requires high electrical conductivity, large Seebeck coefficient, and low thermal conductivity at the same time, which is very difficult to be realized in real materials. In fact, reliable calculations of materials parameters do not give promising results. Since such calculations are done near equilibrium states, we hope that the thermoelectric performance may go beyond theoretical limitations in non-equilibrium states [40, 41]. As such, we are trying to find ways to break through the poor efficiency by focusing non-equilibrium states. In this article, we show our preliminary results for two types of photo-excited thermoelectrics. One is the thermoelectrics using the photo-Seebeck effects (Fig. 1a), and the other is the thermoelectric energy conversion in a

This work was partially supported by ALCA, Japan Science and Technology Agency, and by The Mitsubishi Foundation.

I. Terasaki (✉) · R. Okazaki · P. S. Mondal · Y.-C. Hsieh
Department of Physics, Nagoya University, Nagoya 464-8602, Japan
e-mail: terra@cc.nagoya-u.ac.jp

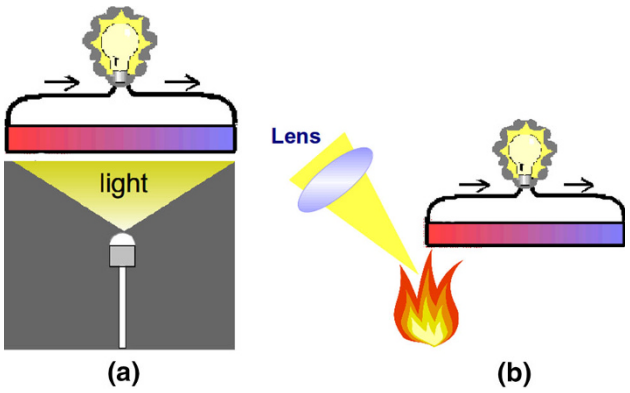

Fig. 1 Schematics of (**a**) power generation using photo-Seebeck effect and (**b**) power generation from focused light

large temperature gradient using solar light as a heat source (Fig. 1b). One may associate the two with photovoltaic and solar-thermal energy conversions.

To emphasize our originality, we will briefly summarize the preceding works. The photo-Seebeck effect was first reported by Tauc [31] in 1955, and was later examined in conventional semiconductors [7, 15]. Note that the word "photo-thermoelectric" is confusing; it stood for the photo-Seebeck effect before the 80s, but is now used as photo-thermal energy conversion through the Seebeck effect (for example, see [2, 12]). To our knowledge, our work is the first trial for the thermoelectric energy conversion using the photo-Seebeck effect. In contrast, the second trial shown in Fig. 1b has been examined by many groups. Originally Telkes [32] examined the concept of solar thermoelectric generator in 1954. Naito et al. [18] designed a power converter using concentrated solar light and achieved a high temperature of 2,200 K in vacuum. Suter et al. [30] fabricated the solar thermoelectric generator and analyzed the efficiency and the maximum power. Fan et al. [3] reported an efficiency of 3 % using commercially available Peltier modules. Thus, our originality lies on the fact that our device is made of *single crystals of transition metal oxide*, which can work at 800 K in air.

Photo-Seebeck effect in oxide single crystals

Although the first observation of the photo-Seebeck effect was reported in the mid 50s [31], there have been very few reports on the photo-Seebeck measurements since the 80s. Thus, we had to newly establish measurement procedure with recently available equipments such as a light-emitting diode (LED). Here, we elaborate on the measurement and analysis details for the photo-Seebeck coefficient, which was not included in the published papers [17, 20].

Commercially available substrates were used as ZnO single crystals, and flux method was employed for making single crystals of PbO. The photoconductivity of ZnO and PbO single crystals was measured with a two-probe method. The thermoelectric voltage of ZnO was measured with two-probe technique with several temperature difference and several photon intensities [20]. The resistance of PbO was too high to use the same measurement setup as in the case of ZnO. Instead, the thermoelectric current was measured with several temperature difference and several photon intensities [17].

The photo-Seebeck effect is a change in the Seebeck coefficient with light illumination, which can be evaluated by comparing the thermoelectric voltage before and after illumination. However, the light illumination affects various properties at the same time; It causes the photovoltaic voltage at the contacts, increases the sample temperature, and changes the temperature difference. To be more quantitative, the measured thermoelectric voltage V_{TE} can be expressed by temperature difference ΔT at dark as

$$V_{\mathrm{TE}} = S\Delta T + V_0, \tag{1}$$

where S is the Seebeck coefficient at dark and V_0 is the offset voltage. When illuminated, the voltage can be written as

$$V_{\mathrm{TE}} = (S + \delta S)(\Delta T + \delta T) + (V_0 + \delta V_0), \tag{2}$$

where δS is the photo-induced change in the Seebeck coefficient. δT and δV_0 are the photo-induced temperature difference and photovoltaic component, respectively. Note that we measured the voltage in a cryostat (Quantum Design PPMS), where the sample temperature was strictly controlled.

The best way to measure the photo-Seebeck coefficient is to measure V_{TE} as a function of $\Delta T + \delta T$. When V_{TE} is found to be a linear function of $\Delta T + \delta T$, the photo-Seebeck coefficient of $S + \delta S$ and the photovoltaic component $V_0 + \delta V_0$ are evaluated from the slope and the intercept, respectively. Figure 2 shows a typical example for the thermoelectric voltage with various photon intensities. The value of I_{LED} represents the input current to an LED of 365 nm and 0 mA corresponds to the dark state. As is clearly shown, the slope systematically decreases with increasing I_{LED}, which means that the Seebeck coefficient decreases in magnitude with light illumination. This is reasonable because the light illumination generates carriers in the sample (photo-doping). Note that the intercept also changes with I_{LED}, which indicates a significant photovoltaic component induced by light illumination. We further comment that the temperature difference changes with I_{LED}. This implies that the absorbed photon is converted into heat, and the heat flows through the sample to the heat bath. If the heat flow is completely homogeneous, the temperature

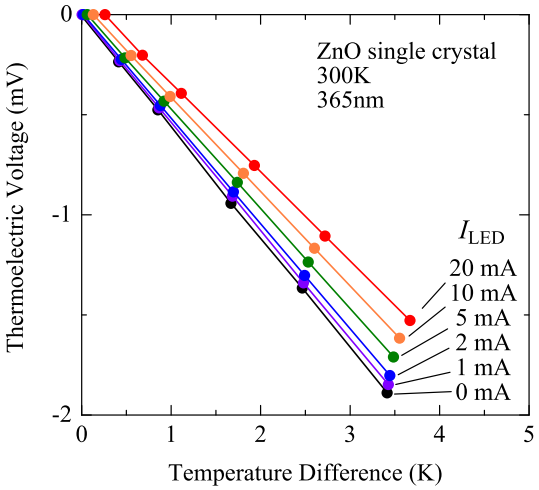

Fig. 2 Thermoelectric voltage in a ZnO single crystal plotted as a function of temperature difference. The LED current I_{LED} corresponds to the photon intensity

difference will be unchanged. Owing to unwanted asymmetry, a finite value of δT is observed.

In the case of PbO, the sample resistance is too high to measure V_{TE} because of the huge Johnson–Nyquist noise. Instead, the thermoelectric current I_{TE} was measured with a pico/femto-ampere meter as a function of temperature difference expressed by

$$I_{TE} = (S + \delta S)(\Delta T + \delta T)/(R - \delta R) + I_0, \quad (3)$$

where R is the sample resistance at dark and δR is the photo-resistance of the sample. Thus, if the photo-resistance is measured in different runs, the thermoelectric voltage is evaluated as $(R - \delta R)I_{TE}$. When $(R - \delta R)I_{TE}$ is a linear function of $\Delta T + \delta T$, the photo-Seebeck coefficient is evaluated from the slope.

Figure 3 shows a typical experimental result in a PbO single crystal. The thermoelectric current I_{TE} is measured as a function of ΔT in Fig. 3a. With increasing I_{LED}, the slope increases rapidly, which is mainly determined by photoconduction. Figure 3b is the thermoelectric voltage plotted as a function of temperature difference, where the slope slightly changes with I_{LED}, indicating photo-Seebeck effect in this oxide. Similarly to ZnO, the results in Fig. 3 can be understood in terms of photo-doping. The type of the carrier is hole in PbO, whereas it is electron in ZnO. It should be noted that chemical doping is quite difficult in PbO, and that light illumination is an effective tool for carrier doping in PbO.

After a phenomenological analysis based on the two-layer model, we have obtained the intrinsic photo-Seebeck coefficient and the intrinsic values of photo-doped carrier density [17, 20]. We find a maximum value for the photo-doped electron density is of the order of 10^{19} cm^{-3}, which is nearly the same value of the optimally doped

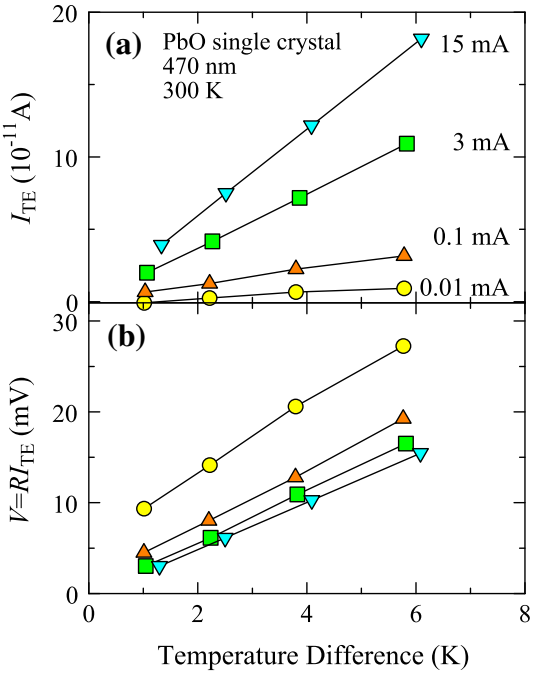

Fig. 3 (**a**) Thermoelectric current I_{TE} and (**b**) thermoelectric voltage RI_{TE} in a PbO single crystal plotted as a function of temperature difference. The *numbers* in mA represent the LED current I_{LED} corresponding to the photon intensity

thermoelectric semiconductors [28]. Thus, we can conclude that the ultraviolet LED can be an alternative carrier source. In the case of PbO, a maximum value is of the order of 10^{18} cm^{-3}, one-order of magnitude smaller than in the case of ZnO.

Thermoelectric uni-couple made of single-crystal oxides

Since the discovery of good thermoelectric properties in the layered cobalt oxide Na_xCoO_2 [33], oxide thermoelectrics has been explored extensively. The layered cobalt oxides are now ready to be applied for thermoelectric power generation, and a prototype power generator is now commercially available at a venture company [1]. All the layered cobalt oxides show good thermoelectric performance at high temperatures. Above 700 K, the thermoelectric performance exceeds a qualifying value (the dimensionless figure of merit larger than unity) in single-crystal samples [5, 6, 25], while it remains a somewhat lower value in ceramic samples [11, 19, 37, 39]. Thus, a device using single crystals is expected to show a better performance than ceramic samples.

We have made a trial device of a uni-couple consisting of single-crystal $Bi_2Sr_2Co_2O_y$ (p-type) and single-crystal $CaMnO_3$ (n-type). Single crystals were grown through a floating-zone technique, and the p–n junction was made

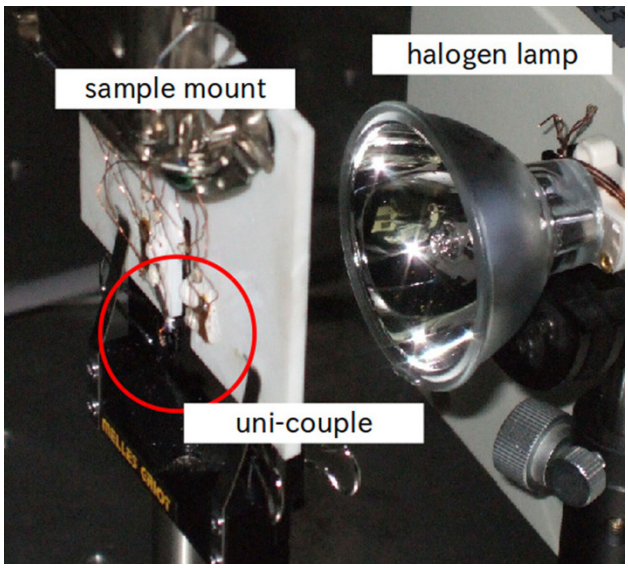

Fig. 4 Power curve measurement setup using halogen lamp as a heat source

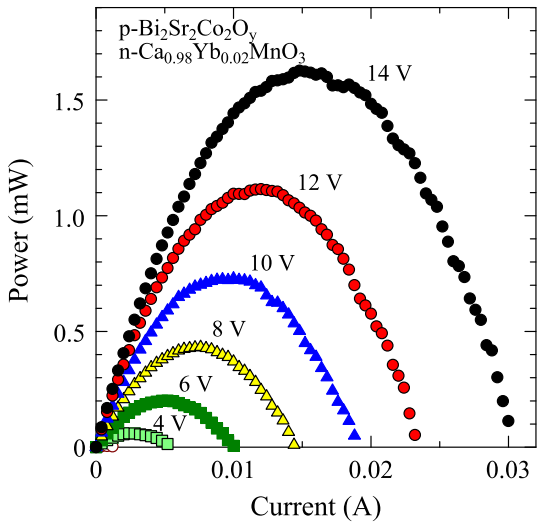

Fig. 5 Power curves of the uni-couple device made of single-crystal oxides. The *numbers* in volt represent the input voltage for the halogen lamp

using silver paint. The dimensions were 1.4 × 1.2 × 9.4 mm^3 for *p*-type and 1.2 × 1.1 × 11 mm^3 for *n*-type. The current–voltage characteristics were measured with a home-made characterization system. A focused halogen light was used as a heat source, and three platinum resistance thermometers were attached at the ends of the device (one at the hot junction and the other two at the cold edges). Figure 4 shows a photographic image of our measurement setup. The device supported on a machinable ceramic plate is set at the focal point of the halogen lamp.

Figure 5 shows typical power curves of the single-crystal uni-couple. Since the device design is not yet optimized, the maximum power output is only 1.5 mW. Although both *p*- and *n*-legs are made of single crystals, the thermoelectric properties are not yet optimized either. In addition, this measurement includes the contact resistance and circuit resistance, which underestimates the power output.

Let us compare the device performance with other oxide devices. Table 1 lists the oxide device performance reported so far. The materials, the operating temperature difference ΔT, and the number of pairs N are different from one to another. The maximum output per pair P_p in our device is comparable with some devices.

One characteristic feature of this device is that a large temperature difference is generated across the sample. Figure 6a shows the hot-side temperature T_H and the cold-side temperature T_C of the uni-couple plotted as a function of the input voltage of the halogen lamp V_{light}. With increasing V_{light}, T_H increases monotonically, while the two T_C's almost stay near room temperature. At a maximum voltage of 14 V, the temperature difference reaches 500 K.

Table 1 Comparison with oxide thermoelectric modules

Reference	Materials	N	ΔT (K)	V_{oc} (mV)	P_{max} (mW)	P_p (mW)
Matsubara et al. [16]	CaGdCoO/ CaMnO	8	773	988	63.5	7.9
Urata et al. [36]	CaCoO/CaMnO	8	973	700	340	42.5
Shin et al. [26]	NaCoCuO/ BaSrPbO	1	506	140	12.0	12.0
Ono et al. [21]	NaCoO/ CaLaMnO	2	166	63	2.3	1.15
Hayashi et al. [8]	LaSrCuO/ NdCeCuO	25	360	1,300	26.3	1.05
Reddy et al. [23]	CaCoO/ CaSmMnO	2	925	400	31.5	17.0
Tomes et al. [35]	LaSrCuO/ CaMnNbO	2	622	46	88.8	44.4
Inagoya et al. [10]	NdCaCoO/ LaCoMnO	10	170	1,010	10.8	1.08
This work	BiSrCoO/ CaYbMnO	1	500	200	1.6	1.6

The number of pairs N, the temperature difference ΔT, the open-circuit voltage V_{oc}, and the maximum power P_{max} are listed. The maximum power per pair $P_p = P_{max}/N$ is also listed

Since the device length is approximately 1 cm, the temperature gradient reaches a large value of 500 K/cm by air-cooling without blower.

Owing to the large temperature difference, thermoelectric parameters change within the device though their temperature dependence. Snyder and Ursell [29] have found the exact expression for the conversion efficiency that is valid even in such conditions. Surprisingly, the efficiency is determined only by the values at the high and

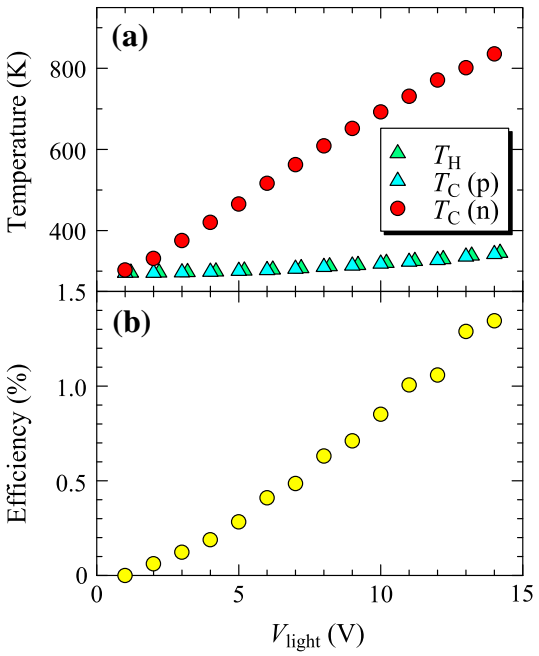

Fig. 6 (**a**) The temperatures at the hot edge T_H and the temperatures at the cold edges T_C's (**b**) the conversion efficiency calculated by Eq. (4) plotted as a function of the input voltage for the halogen lamp V_{light}

low temperature edges of the device. A concrete form of the expression is given by

$$\eta = 1 - \frac{S_C T_C + 1/u_C}{S_H T_H + 1/u_H}, \quad (4)$$

where the subscripts of H and C represent the values at the hot and cold edges. The quantity of $u \equiv j/\kappa\nabla T$ is called the relative current density, which is the ratio of the electrical current density to the heat flux density by thermal conduction.

The temperatures (T_H and T_C) at the cold and hot edges were monitored in the power curve measurements. The Seebeck coefficients (S_H and S_C) at the cold and hot edges were known by measuring the Seebeck coefficients of *p*- and *n*-type crystals in advance. To calculate the relative current density, the resistivity and the thermal conductivity are necessary. The resistivity values were measured for the prepared crystals, and the thermal conductivity data were taken from the literature [4, 24]. Figure 6b shows the conversion efficiency plotted as a function of V_{light}. The maximum efficiency is a reasonably large value of 1.4 % in spite of the fact that all the conditions were far from ideal. The present measurement is a first step for this kind of thermoelectric power generator, and we notice many issues to improve the device performance. Kraemer et al. [14] have reported an efficiency of 4.6 % in a solar thermoelectric generators using Bi_2Te_3-based device. Although the device concept is completely different from our device, we preliminarily obtained a similar efficiency in another modified uni-couple (not shown).

An advantage of oxide device is seen in the smooth evolution of the power curves in Fig. 5. This implies that the device resistance is almost constant from 300 to 800 K, and the device is sufficiently stable at 800 K in air. Considering that the surface temperature at the focal point on the device is much higher, we think that this experiment demonstrates the high-temperature stability of oxide devise in air.

We are considering a possibility to use this type of device to the black-body radiation from high-temperature furnace. Recalling that the sun is a black body of 6,000 K, we can use black-body radiation from other hot sources as well. For example, a black body of 1,000 K will give a large photon flux of 57 kW/m^2, being 50 times larger than that of the sun. Heat is difficult to control; It is hardly stored, transported or accumulated at our disposal, but electromagnetic wave can be done so.

Summary and future prospects

In this article, we have reported our attempts to find a better thermoelectric power generation using light. One approach is the thermoelectrics using the photo-Seebeck effect. We have shown the *n*-type photo-Seebeck effect in ZnO and the *p*-type one in PbO. Although the thermoelectric energy conversion is not yet done, the photo-doping gives reasonably good thermoelectric parameters. The second approach is the thermoelectric energy conversion using focused light as a heat source. The device structure and thermoelectric materials are not yet optimized, and the efficiency is 1.4 % at the present stage. Nevertheless, we have successfully shown the high-temperature stability of the oxide device, and also shown that the oxide thermoelectric uni-couple can be made from single crystals. The former approach uses ultraviolet light for a doping tool, while the latter uses infrared light as a heat source. Since these two lights are not used in Si-based solar cells, our two approaches can live with solar cells to increase the total energy conversion efficiency. Actually, Park et al. [22] and Wang et al. [38] already have combined an existing photovoltaic cell with a thermoelectric module. We look forward to developing a new device making full use of solar energy by combining photovoltaics with thermoelectrics, even though we cannot see the concrete shape at the moment.

Acknowledgments We would like to thank A. Horikawa for her tenacious efforts to establish measurement procedure for the photo-Seebeck effect. We also wish to thank Y. Yasui, H. Taniguchi, M. Fujita, and Y. Shiraishi for close collaboration of this work. We also appreciate R. Funahashi and H. Ohta for fruitful discussion.

References

1. TES New Energy corporation (2010). http://tes-ne.com/English/01_home_e.html
2. Basko, D.: A photothermoelectric effect in graphene. Science **334**(6056), 610–611 (2011). doi:10.1126/science.1214560
3. Fan, H., Singh, R., Akbarzadeh, A.: Electric power generation from thermoelectric cells using a solar dish concentrator. J. Electr. Mater. **40**(5), 1311–1320 (2011). doi:10.1007/s11664-011-1625-x
4. Flahaut, D., Mihara, T., Funahashi, R., Nabeshima, N., Lee, K., Ohta, H., Koumoto, K.: Thermoelectrical properties of A-site substituted $Ca_{1-x}Re_xMnO_3$ system. J. Appl. Phys. **100**(8), 084911 (2006). doi:10.1063/1.2362922
5. Fujita, K., Mochida, T., Nakamura, K.: High-temperature thermoelectric properties of $Na_xCoO_{2-\delta}$ single crystals. Jpn. J. Appl. Phys. **40**(Part 1, No. 7), 4644–4647 (2001). doi:10.7567/JJAP.40.4644
6. Funahashi, R., Shikano, M.: $Bi_2Sr_2Co_2O_y$ whiskers with high thermoelectric figure of merit. Appl. Phys. Lett. **81**(8), 1459–1461 (2002). doi: 10.1063/1.1502190
7. Harper, J.G., Matthews, H.E., Bube, R.H.: Two-carrier photothermoelectric effects in GaAs. J. Appl. Phys. **41**(7), 3182–3184 (1970). doi:10.1063/1.1659387
8. Hayashi, S.F., Nakamura, T., Kageyama, K., Takagi, H.: Monolithic thermoelectric devices prepared with multilayer cofired ceramics technology. Jpn. J. Appl. Phys. **49**(9), 096505 (2010). doi:10.7567/JJAP.49.096505
9. He, J., Liu, Y., Funahashi, R.: Oxide thermoelectrics: the challenges, progress, and outlook. J. Mater. Res. **26**(15), 1762–1772 (2011). doi:10.1557/jmr.2011.108
10. Inagoya, A., Sawaki, D., Horiuchi, Y., Urata, S., Funahashi, R., Terasaki, I.: Thermoelectric module made of perovskite cobalt oxides with large thermopower. J. Appl. Phys. **110**(12), 123712 (2011). doi:10.1063/1.3671070
11. Ito, M., Nagira, T., Furumoto, D., Katsuyama, S., Nagai, H.: Synthesis of $Na_xCo_2O_4$ thermoelectric oxides by the polymerized complex method. Scripta Mater. **48**(4), 403–408 (2003). doi: 10.1016/S1359-6462(02)00443-8
12. Kasymakhunova, A., Nabiev, M.: Photothermoelectric converters of concentrated radiation. Tech. Phys. Lett. **29**(3), 253–255 (2003). doi:10.1134/1.1565650
13. Koumoto, K., Wang, Y., Zhang, R., Kosuga, A., Funahashi, R.: Oxide thermoelectric materials: a nanostructuring approach. Ann. Rev. Mater. Res. **40**(1), 363–394 (2010). doi:10.1146/annurev-matsci-070909-104521
14. Kraemer, D., Poudel, B., Feng, Hp, Caylor, J.C., Yu, B., Yan, X., Ma, Y., Wang, X., Wang, D., Muto, A., McEnaney, K., Chiesa, M., Ren, Z., Chen, G.: High-performance flat-panel solar thermoelectric generators with high thermal concentration. Nat. Mater. **10**, 532–538 (2011). doi:10.1038/nmat3013
15. Kwok, H.B., Bube, R.H.: Thermoelectric and photothermoelectric effects in semiconductors: CdS single crystals. J. Appl. Phys. **44**(1), 138–144 (1973). doi:10.1063/1.1661848
16. Matsubara, I., Funahashi, R., Takeuchi, T., Sodeoka, S., Shimizu, T., Ueno, K.: Fabrication of an all-oxide thermoelectric power generator. Appl. Phys. Lett. **78**(23), 3627–3629 (2001). doi:10.1063/1.1376155
17. Mondal, P.S., Okazaki, R., Taniguchi, H., Terasaki, I.: Photo-seebeck effect in tetragonal PbO single crystals. J. Appl. Phys. **114**(17), 173710 (2013). doi:10.1063/1.4829460
18. Naito, H., Kohsaka, Y., Cooke, D., Arashi, H.: Development of a solar receiver for a high-efficiency thermionic/thermoelectric conversion system. Sol. Energy **58**(4–6), 191–195 (1996). doi:10.1016/S0038-092X(96)00084-9
19. Ohtaki, M., Nojiri, Y., Maeda, E.: Improved thermoelectric performance of sintered $NaCo_2O_4$ with enhanced 2-dimensional microstructure. In: Rowe, M. (ed.) Proceedings of The 19th International Conference on Thermoelectrics (ICT2000), pp. 190–195. Babrow, Cardiff (2000)
20. Okazaki, R., Horikawa, A., Yasui, Y., Terasaki, I.: Photo-seebeck effect in ZnO. J. Phys. Soc. Jpn. **81**(11), 114722 (2012). doi:10.1143/JPSJ.81.114722
21. Ono, Y., Kimura, D., Kawano, S.H.O., Watanabe, R., Kajitani, T.: Fabrication and performance of an oxide thermoelectric power generator. In: Proceedings of The 21st International Conference on Thermoelectrics (ICT2002), pp. 454–457. IEEE (2002)
22. Park, K.T., Shin, S.M., Tazebay, A.S., Um, H.D., Jung, J.Y., Jee, S.W., Oh, M.W., Park, S.D., Yoo, B., Yu, C., Lee, J.H.: Lossless hybridization between photovoltaic and thermoelectric devices. Sci. Rep. **3**, 2123 (2013). doi:10.1038/srep02123
23. Reddy, E.S., Noudem, J.G., Hebert, S., Goupil, C.: Fabrication and properties of four-leg oxide thermoelectric modules. J. Phys. D **38**(19), 3751–3755 (2005). doi:10.1088/0022-3727/38/19/026
24. Satake, A., Tanaka, H., Ohkawa, T., Fujii, T., Terasaki, I.: Thermal conductivity of the thermoelectric layered cobalt oxides measured by the Harman method. J. Appl. Phys. **96**(1), 931–933 (2004). doi:10.1063/1.1753070
25. Shikano, M., Funahashi, R.: Electrical and thermal properties of single-crystalline $(Ca_2CoO_3)_{0.7}CoO_2$ with a $Ca_3Co_4O_9$ structure. Appl. Phys. Lett. **82**(12), 1851–1853 (2003). doi: 10.1063/1.1562337
26. Shin, W., Murayama, N., Ikeda, K., Sago, S., Terasaki, I.: Thermoelectric device of $Na(Co, Cu)_2O_4$ and $(Ba, Sr)PbO_3$. J. Cer. Soc. Jpn. **110**(8), 727–730 (2002). doi: 10.2109/jcersj.110.727
27. Singh, G.: Solar power generation by PV (photovoltaic) technology: a review. Energy **53**, 1–13 (2013). doi:10.1016/j.energy.2013.02.057
28. Snyder, G.J., Toberer, E.S.: Complex thermoelectric materials. Nat. Mater. **7**, 105–114 (2008). doi:10.1038/nmat2090
29. Snyder, G.J., Ursell, T.S.: Thermoelectric efficiency and compatibility. Phys. Rev. Lett. **91**(14), 148301 (2003). doi:10.1103/PhysRevLett.91.148301
30. Suter, C., Tomes, P., Weidenkaff, A., Steinfeld, A.: Heat transfer and geometrical analysis of thermoelectric converters driven by concentrated solar radiation. Materials **3**(4), 2735–2752 (2010). doi:10.3390/ma3042735
31. Tauc, J.: The thermal photo-electric phenomenon in semi-conductors. Czech. Phys. J. **5**(4), 528–535 (1955). doi:10.1007/BF01687219
32. Telkes, M.: Solar thermoelectric generators. J. Appl. Phys. **25**(6), 765–777 (1954). doi:10.1063/1.1721728
33. Terasaki, I., Sasago, Y., Uchinokura, K.: Large thermoelectric power in $NaCo_2O_4$ single crystals. Phys. Rev. B **56**(20), R12685–R12687 (1997). doi: 10.1103/PhysRevB.56.R12685
34. Thirugnanasambandam, M., Iniyan, S., Goic, R.: A review of solar thermal technologies. Renew. Sustain. Energy Rev. **14**(1), 312–322 (2010). doi:10.1016/j.rser.2009.07.014
35. Tomes, P., Trottmann, M., Suter, C., Aguirre, M.H., Steinfeld, A., Haueter, P., Weidenkaff, A.: Thermoelectric oxide modules (TOMs) for the direct conversion of simulated solar radiation into electrical energy. Materials **3**(4), 2801–2814 (2010). doi:10.3390/ma3042801
36. Urata, S., Funahashi, R., Mihara, T., Kosuga, A., Sodeoka, S., Tanaka, T.: Power generation of a p-type $Ca_3Co_4O_9$/n-type $CaMnO_3$ module. Int. J. Appl. Cer. Technol. **4**(6), 535–540 (2007). doi: 10.1111/j.1744-7402.2007.02173.x

37. Van Nong, N., Pryds, N., Linderoth, S., Ohtaki, M.: Enhancement of the thermoelectric performance of *p*-type layered oxide $Ca_3Co_4O_{9+d}$ through heavy doping and metallic nanoinclusions. Adv. Mater. **23**(21), 2484–2490 (2011). doi: 10.1002/adma.201004782
38. Wang, N., Han, L., He, H., Park, N.H., Koumoto, K.: A novel high-performance photovoltaic–thermoelectric hybrid device. Energy Environ. Sci. **4**(9), 3676–3679 (2011). doi:10.1039/c1ee01646f
39. Wang, Y., Sui, Y., Cheng, J., Wang, X., Su, W.: Comparison of the high temperature thermoelectric properties for Ag-doped and Ag-added $Ca_3Co_4O_9$. J. Alloys Comp. **477**(1–2), 817–821 (2009). doi: 10.1016/j.jallcom.2008.10.162
40. Whitney, R.S.: Nonlinear thermoelectricity in point contacts at pinch off: a catastrophe aids cooling. Phys. Rev. B **88**(6), 064302 (2013). doi:10.1103/PhysRevB.88.064302
41. Zebarjadi, M., Esfarjani, K., Shakouri, A.: Nonlinear peltier effect in semiconductors. Appl. Phys. Lett. **91**(12), 104122 (2007). doi:10.1063/1.2785154